MEMORANDUM
RM-3490-PR
MAY 1965

AD617549

THE ROLE C
MELTING AND VAPORIZATION I
HYPERVELOCITY IMPAC

R. L. Bjork and A. E. Olsha

The RAND Corporation
SANTA MONICA · CALIFORNIA

THE ROLE OF
MELTING AND VAPORIZATION IN
HYPERVELOCITY IMPACT

R. L. Bjork and A. E. Olshaker

The RAND Corporation
1700 MAIN ST · SANTA MONICA · CALIFORNIA · 90406

Approved for OTS release

PREFACE

For several years RAND has conducted a study of hypervelocity impact. Applications of the results have been made to the problems of the meteoroid hazard, satellite vulnerability, and ICBM defense. This Memorandum discusses the effects which shock-induced melting and vaporization have upon the impact process.

SUMMARY

This Memorandum discusses the thermodynamics associated with the flow processes in hypervelocity cratering.

Qualitative, graphical arguments are presented to show that previously proposed thermal-impact theories, which postulate that the kinetic energy of impacting projectiles goes entirely into breaking of chemical bonds or fusion, considerably overestimate the transference of energy into heating.

The work conducted at Los Alamos on the evaluation of release temperatures and phases of nine metals as a function of shock strength is summarized, and similar information is estimated for ten additional metals. The data on release temperature as a function of maximum shock pressure provide a basis for calculating the threshold impact velocities of various projectiles that cause incipient and complete melting in the target material. These calculations were carried out and the results are tabulated for 19 target materials which are impacted by iron and aluminum projectiles as well as by projectiles of the same material as the targets. Examination of the tabulated data indicates that the fraction of maximum shock internal energy remaining in the target on release is approximately constant. This empirical fact is employed to predict additional data.

The results indicate that a quantitative evaluation of the effects of heating in an impact process requires a detailed knowledge of the maximum shock pressures as a function of position within the target. Such an evaluation is made for the case of an aluminum projectile impacting an aluminum target at 20 km/sec, based upon the earlier results of one of the authors. It is shown that the heating effects enhance the validity of the hydrodynamic model and must be considered in any theoretical prediction of an impact crater. At lower impact velocities this heating modifies the material strength, and at high impact velocities it creates a melted region in the target which has greater dimensions than the crater size originally predicted on the basis of hydrodynamic flow only.

CONTENTS

SYMBOLS

C_p = constant-pressure heat capacity

C_v = constant-volume heat capacity

e = specific internal energy

f = fraction of maximum shock internal energy remaining in material as "heat" energy

H_m = specific internal energy at incipient melting under zero pressure

K = isothermal compressibility

Mb = megabars

P = pressure

S = entropy

T = temperature

V = velocity

v = specific volume

β = volume coefficient of thermal expansion

γ = Gruneisen ratio

Subscripts

F = final conditions

H = conditions on the Hugoniot

m = melting conditions

O = initial, ambient conditions

I.   INTRODUCTION

During the portion of the hypervelocity impact wherein the material
is severely compressed and under tremendous pressures, the state (solid,
liquid, or gas) of the material does not play a very important role.
The shear stress that the material can support is so small compared with
the pressures generated, and the heats of fusion and vaporization are
so small compared with the specific internal energies which appear, that
these factors cannot affect the process in an important way. However,
in the later stages of the process, when the pressures and specific in-
ternal energies fall to low levels, the condition of the material can
become important. One should focus his attention on the state to which
the material reverts after the severe compression, when expansion back
to low pressure has occurred. It is not necessary to devote much atten-
tion to the precise point at which phase changes occur during the expan-
sion, which is fortunate, since the determination of this information is
very difficult.

If the material were compressed adiabatically and then expanded
adiabatically, there would be little residual heating. However, in an
impact process the material is first compressed by a shock, and in this
process the entropy is raised. In the subsequent adiabatic expansion
the entropy is unchanged, so that on returning to low pressure the ma-
terial has a greater entropy than it began with. It can be shown quite
generally that the entropy excess initially increases rapidly with shock
strength, depending on the third and higher powers of shock strength.[1]
Shocks of low strength will leave the material in the solid state, but
heated to some degree. Stronger and stronger shocks lead to fusion,
heated liquid, vaporization, and superheated vapor as the final state.
The aim in this Memorandum is to discuss the final condition of the ma-
terial as a function of shock strength, and to illustrate some effects
on the hypervelocity-impact process.

II.   THERMODYNAMICS OF SHOCK FLOW

The shock-compression process for any material is described by a curve in the pressure-volume plane which is known as the Hugoniot curve. Since the shock process is an abrupt and irreversible one, the Hugoniot curve indicates only the locus of points to any one of which the shock of that particular strength abruptly brings the material from a pre-scribed initial state, and it does not imply a continuous path leading to the final shock pressure. The name of the curve comes from the fact that the relation

$$e_H = \frac{P_H}{2} (v_0 - v_H) \tag{1}$$

which was first derived by Hugoniot in 1889, is identically satisfied between any point on the Hugoniot curve and the initial conditions, which in this case are taken to be $e_o = P_o = 0.$[1] Here e is the specific internal energy; P, the pressure; v, the specific volume; and the subscript H denotes conditions on the Hugoniot.

This equation, which follows from the conservation of mass, momentum, and energy across a shock, can be interpreted as saying that the increase of internal energy across the shock is due to the work done by the mean pressure in performing the compression. It shows that knowledge of the P-v Hugoniot curve determines also the total internal energy at the shock front, including that portion due to irreversible heating.

Precise Hugoniot curves for 27 metals have been experimentally measured by the Los Alamos Laboratories as part of a thorough investigation of the high-pressure behavior of matter which has been under way since 1945.[2,3,4]

Figure 1 schematically illustrates the shock-compression and subsequent expansion processes. Point 1 is on the Hugoniot curve--it represents the state of the material at that shock strength. Equation (1) shows that the total specific internal energy of the material at this pressure is just equal to the area of the dashed triangle. The expansion process back to zero pressure is reversible and adiabatic,
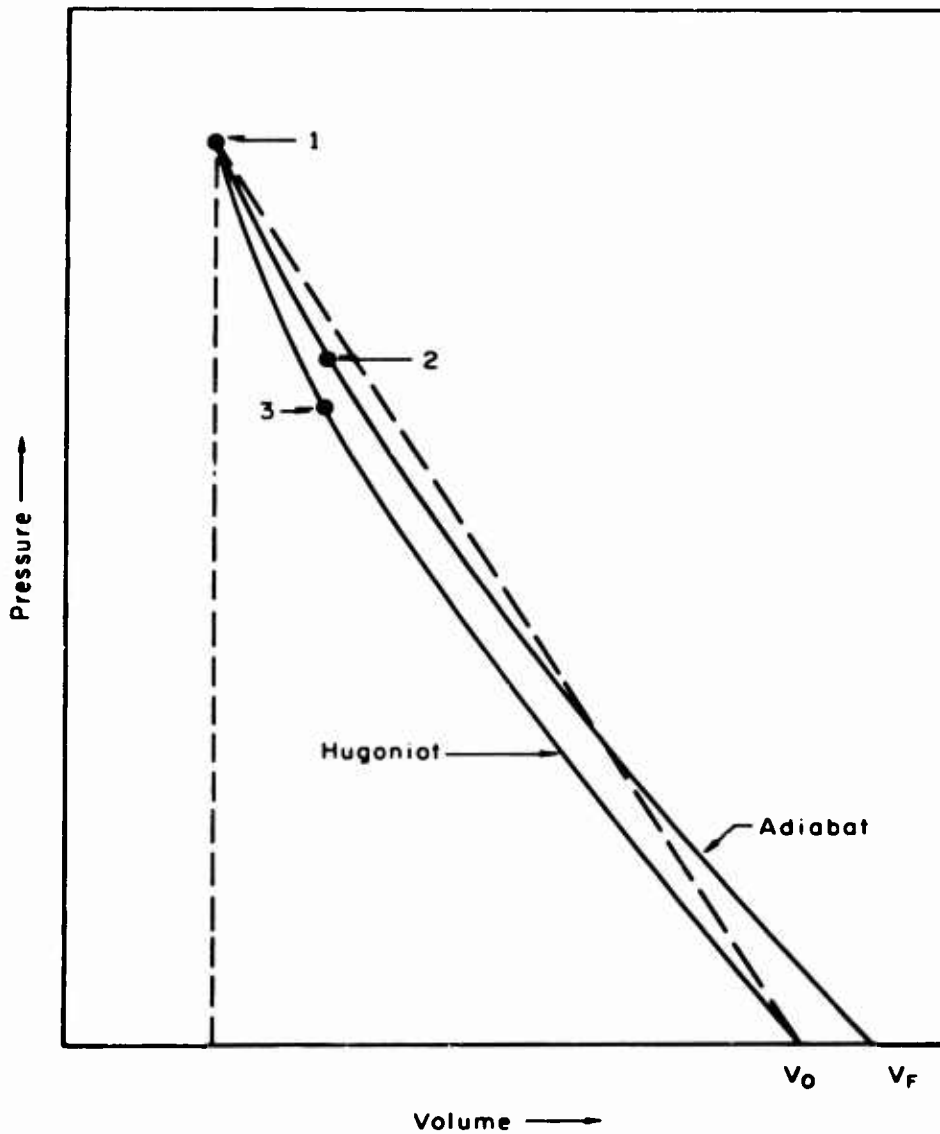
Fig. 1—Qualitative relationship of Hugoniot and adiabat,
illustrating method of calculating internal
energy after shock release

returning the material to a final increased volume as the result of
thermal expansion due to the irreversible heating of the shock process.
The energy that is given up by the material to its surroundings in the
Pdv expansion work is just the area under the adiabatic curve. Because
of the irreversible losses in the shock, this energy is less than the
initial Hugoniot energy--the area under the adiabat is less than the
area of the dashed triangle. It is the difference between these areas
which represents the net energy of heating, and as the figure indicates,
this difference is small compared with the total energies involved.
Therefore, it is seen that those theories which postulate kinetic energy
of impact going entirely into melting, or "breaking of chemical bonds,"
considerably overestimate the transference of energy into residual heat-
ing, since they neglect the work of expansion.

Calculation of expansion adiabats from initial compressions on the
Hugoniot curve is possible if the equation of state is known in the form
$P(v,e)$. The fact that the pressure, volume, and energy relations are
accurately known along the experimentally determined Hugoniot makes the
Mie-Gruneisen equation of state, taken from statistical mechanics, a
reasonable first approximation near the Hugoniot. This formulation is
a natural one for these problems because it is expressed in terms of
pressure and energy increments relative to some base curve, which in
this case is taken to be the Hugoniot; and in the shock-compression and
subsequent expansion problems, variations in the thermodynamic proper-
ties occur in the vicinity of the Hugoniot if the shock is not too
strong. The Mie-Gruneisen equation of state has the form

$$P - P_H = \frac{\gamma}{v} (e - e_H) \qquad (2)$$

where the dimensionless quantity γ is the Gruneisen ratio, which ex-
presses the change of frequency of the thermally oscillating atoms in
a crystal as a function of compression; γ is assumed to be a function
of volume only.[3,4]

An approximation of the variation in γ with volume may be calcula-
ted from the Hugoniot data by relations from statistical mechanics.
The relation employed by Los Alamos for this computation is the Dugdale-

MacDonald equation.[4] The fact that this calculation also provides
an estimate of the absolute value of the Gruneisen ratio at the ini-
tial conditions of zero pressure permits a test of the Gruneisen ap-
proximation, since at zero pressure γ is deducible from thermodynamics
by the following argument: P_H and e_H are on the Hugoniot and are
therefore functions of volume only, as is γ by definition. Therefore,
differentiating Eq. (2) with respect to temperature at constant volume

$$\left(\frac{\partial P}{\partial T}\right)_v = \frac{\gamma}{v}\left(\frac{\partial e}{\partial T}\right)_v \tag{3}$$

But $(\partial e/\partial T)_v = C_v$, the heat capacity at constant volume, and
$(\partial P/\partial T)_v = (\beta/K)$ where $\beta = (1/v)(\partial v/\partial T)_P$, the volume coefficient of
thermal expansion at constant pressure, and $K = -(1/v)(\partial v/\partial P)_T$, the
isothermal compressibility. Therefore

$$\frac{\gamma}{v} = \frac{\beta}{KC_v} \tag{4}$$

is the relation between the Gruneisen equation of statistical mechanics
and the bulk thermodynamics of a crystal.

        The agreement between this value of γ calculated from thermodyna-
mic constants and that calculated from the Dugdale-MacDonald equation
by use of the Hugoniot data is good for 12 metals and lends some con-
fidence to the use of the Mie-Gruneisen equation at zero pressure. For
example, in copper the thermodynamic and Dugdale-MacDonald zero-pressure
values of γ are 2.00 and 1.99, respectively. (One atmosphere is con-
sidered indistinguishable from zero pressure on the scale of pressures
of interest here.) For the three metals gold, lead, and chromium, how-
ever, the zero-pressure agreement is not good. For lead, the Dugdale-
MacDonald equation leads to $\gamma = 2.03$, while the thermodynamic param-
eters imply $\gamma = 2.77$. For these three metals the values of γ/v are
assumed to be constant at the zero-pressure thermodynamic values, and
in fact this is not far from what the theoretical Dugdale-MacDonald
variations yield for the other metals. Figure 2 shows typical values
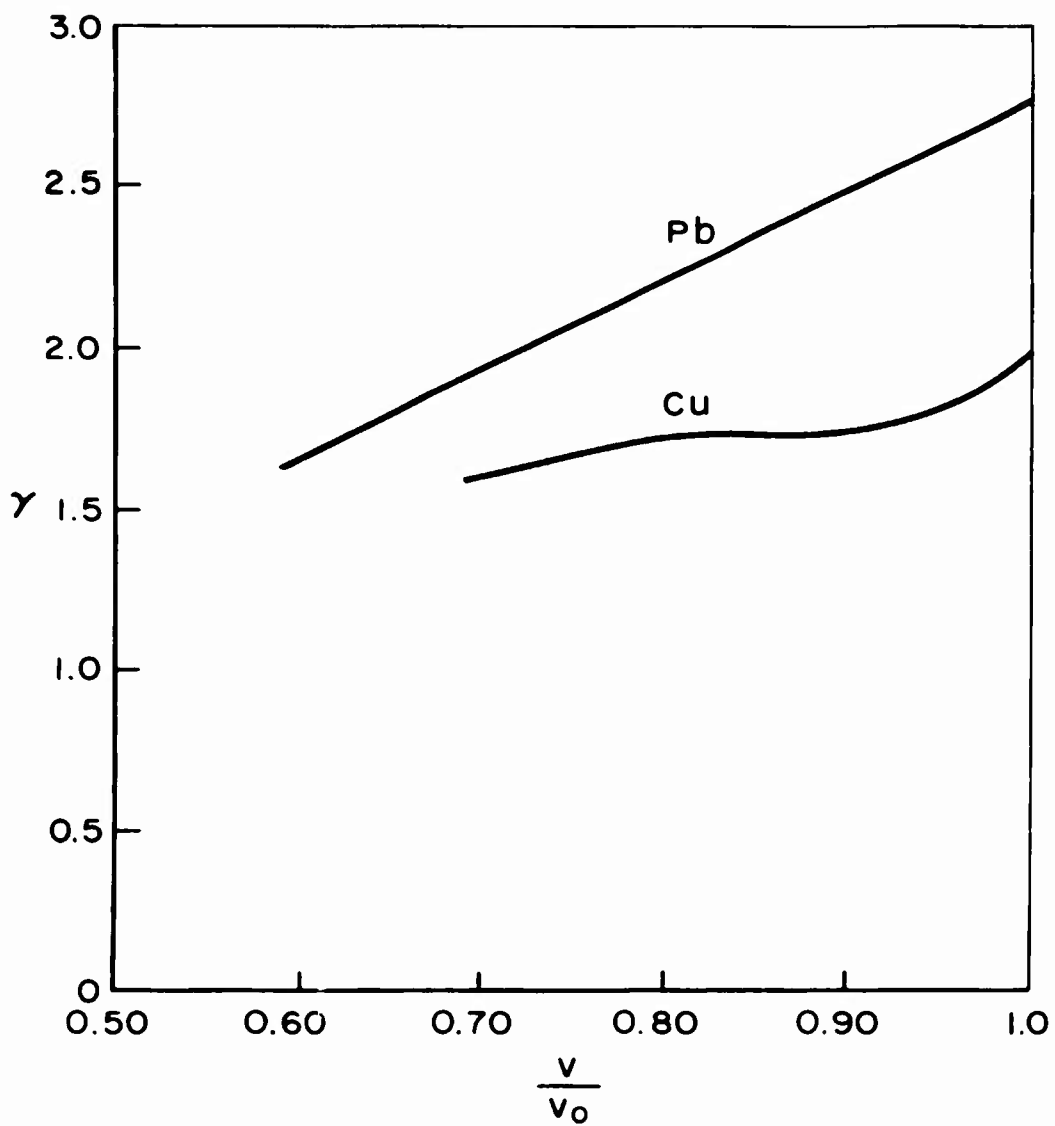of γ resulting from these calculations.

Fig. 2—Gruneisen ratio as a function of volume
for lead and copper

Knowing γ as a function of volume provides a complete description of the equation of state near the Hugoniot. This knowledge permits an integration of the differential equations specifying the isentrope, namely

$$\frac{de}{dv} = -P(v,e) \tag{5}$$

Starting from any point on the Hugoniot, Eq. (5) may be integrated down to zero pressure; the energy and volume corresponding to zero pressure then specify the release internal energy and final volume of the material which has been subjected to a shock and then is released adiabatically to zero pressure. Since the heat capacity at zero pressure (1-atm pressure is sufficiently close to zero for our purposes here) is known as a function of temperature, the specification of the release internal energy allows the calculation of the release temperature. That is, the state (P_F, V_F) could be produced by either the shock-expansion process just described or simple heating at zero pressure from V_0 to V_F. Thus, the expression

$$e_F - e_0 = \int_{T_0}^{T_F} C_P(T)\,dT \tag{6}$$

permits the calculation of T_F from the given value of e_F ($C_P = C_v$ at zero pressure).

III.   IMPACT MELTING OF NINETEEN METALS

By the above methods, Los Alamos workers have calculated the final
release temperatures associated with their experimental shock pressures
for 19 metals.[3]   Figure 3 exhibits, for four metals, these zero-pres-
sure temperatures as a function of the shock pressures from which they
have expanded. The flat portions of the curves are the regions in which
the excess energy is devoted to melting a larger fraction of the mate-
rial instead of raising the temperature. Therefore, the shock pressure
at the left of the flat section is that which just causes incipient
melting, while that at the right is the pressure which just causes
complete melting. The experimental measurements on the copper curve
are those by Taylor.[5]

Table 1 presents these two shock pressures and the associated im-
pact velocities for the nine metals whose fusion takes place within the
Los Alamos experimental pressure range. The velocities of steel and
aluminum projectiles which produce the same thermal effects are added
for convenience in comparing these numbers with experimental impact
conditions in which these projectiles are often employed.[*]   It is in-
teresting to note that the behavior of thallium is quite similar to
that of lead with respect to the properties shown in this table.

For cobalt, chromium, molybdenum, nickel, titanium, vanadium, and
tungsten, the maximum Los Alamos experimental pressures are below those
needed to produce melting. However, a rough estimate of the incipient-
melting shock pressures and impact velocities can be obtained for these
seven metals by extrapolations of the Los Alamos data. Figure 4 is a
plot of release temperature versus shock pressure showing the represen-
tative extrapolations for three metals. The solid curves indicate the
region of the Los Alamos experiments, and the dashed lines extend the
curves to the melting temperatures. Once the melting shock pressures
are obtained by this construction, the impact velocities associated
with these pressures may be obtained by extrapolating the Hugoniot

---

[*]The graphical method of shock solution which furnishes these ve-
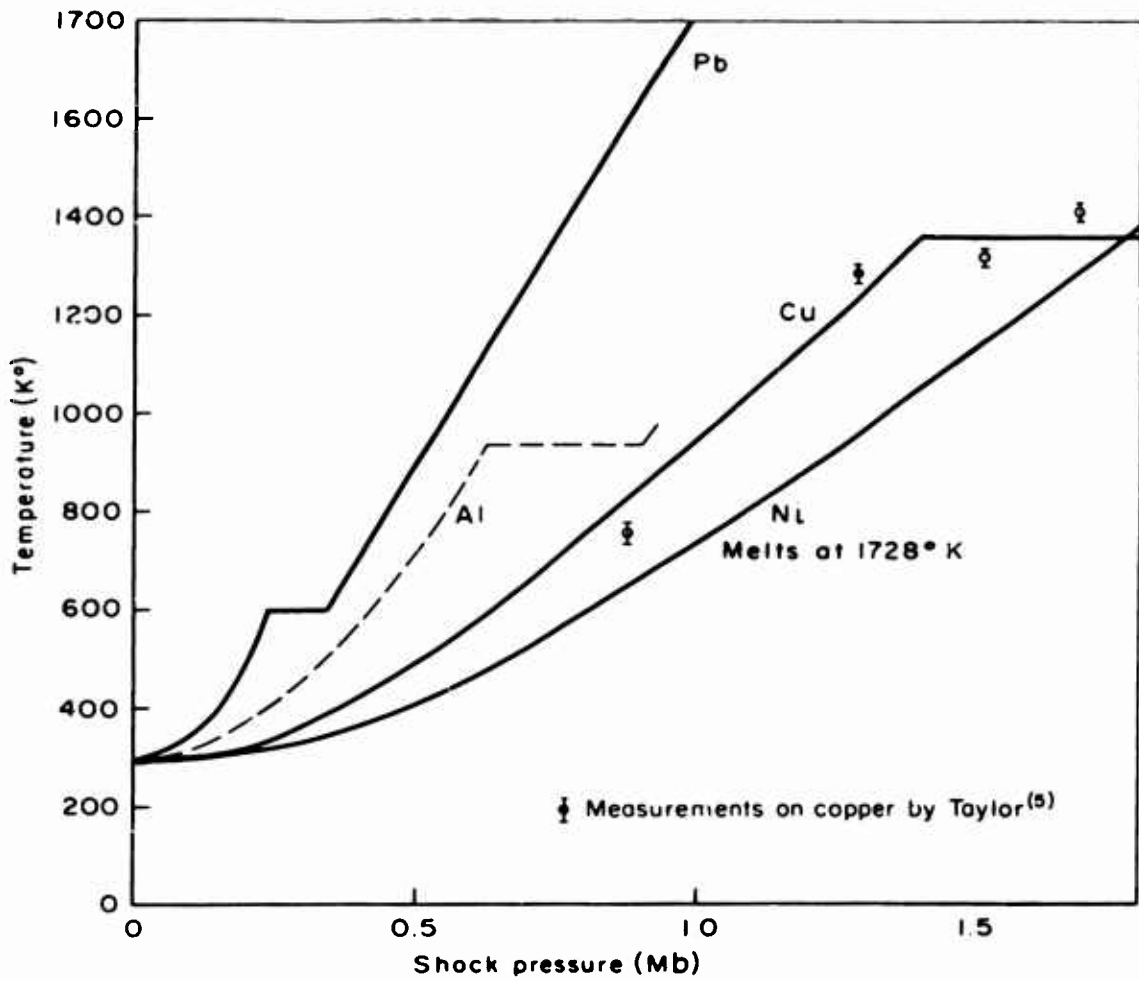locities is discussed in Ref. 6.

Fig. 3—Shock-release temperatures for four metals

Table 1

SHOCK-MELTING PROPERTIES OF NINE METALS[3][a]

Material	Density (gm/cc)	Melting Temp. (°K)	Shock Press. (Mb)		Impact Velocity (km/sec)					
					Similar Material		Iron Projectile		Aluminum Projectile	
			Incip.	Comp.	Incip.	Comp.	Incip.	Comp.	Incip.	Comp.
Gold	19.24	1336	1.46	2.15[b]	2.88	3.7[b]	3.8	4.9[b]	6.0	7.8[b]
Lead	11.34	601	0.25	0.35	1.42	1.8	1.3	1.8	2.0	2.6
Silver	10.49	1234	0.98	1.27[b]	3.22	3.8[b]	3.4	4.1[b]	5.1	6.1[b]
Copper	8.90	2356	1.40	1.84[b]	4.36	5.2[b]	4.5	5.4[b]	6.6	8.0[b]
Cadmium	8.64	594	0.33	0.46	1.90	2.4	1.8	2.3	2.5	3.2
Thallium	11.84	577	0.23	0.30	1.4	1.6	1.3	1.6	2.0	2.3
Thorium	11.68	1968	0.74	0.86	3.1	3.4	3.1	3.4	4.4	4.9
Tin	7.28	505	0.22	0.35	1.56	2.2	1.3	2.0	1.8	2.8
Zinc	7.14	693	0.50	0.70	2.72	3.4	2.5	3.2	3.5	4.5

[a]Additional data received in a personal communication from F. Harlow.
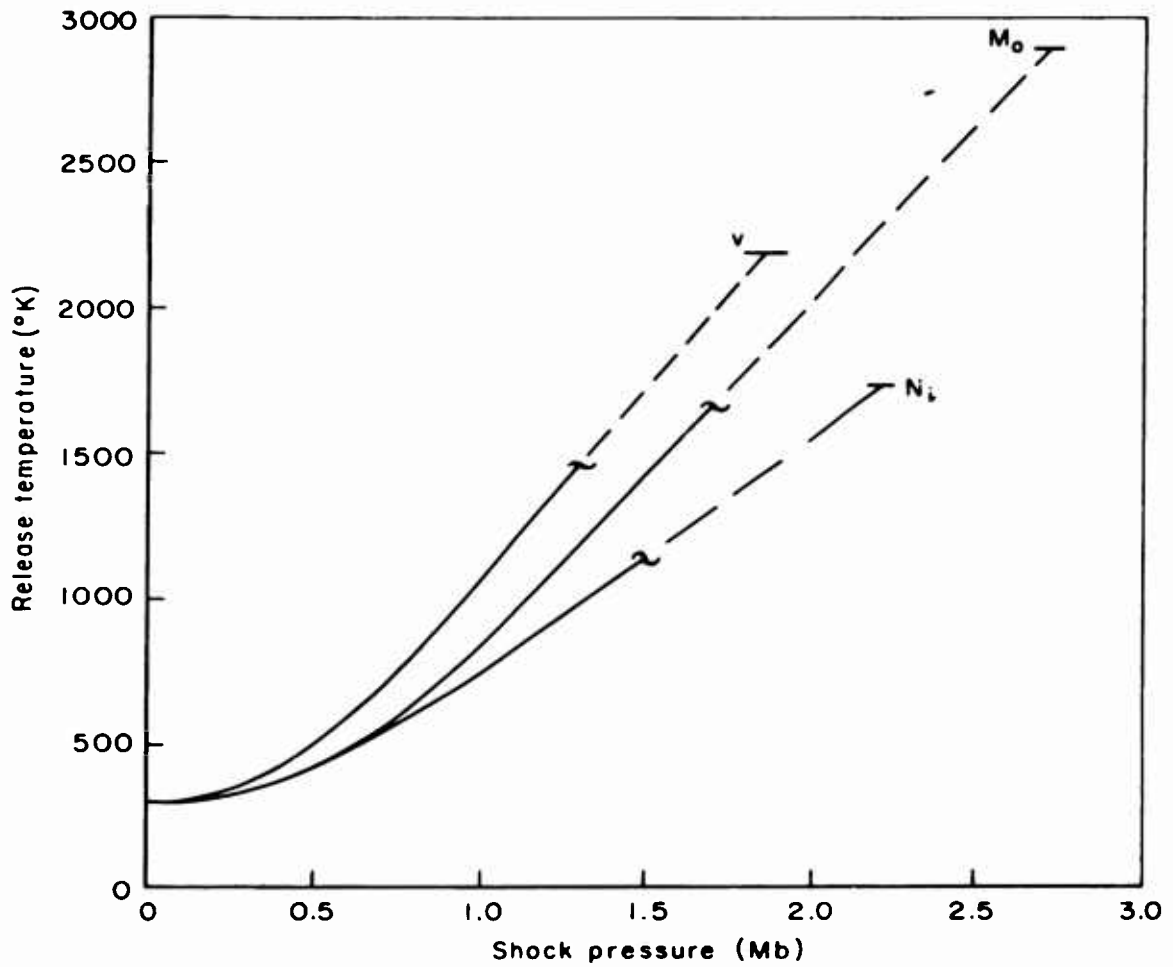[b]Estimated (see Section IV).

Fig. 4—Typical extrapolations of release temperature
versus shock pressure

curves to the melting pressures. The Hugoniot extrapolations may be employed with a much greater degree of confidence than the relatively crude extrapolations of release temperature which are shown in Fig. 4.[3]

The results of these extrapolations, giving approximate incipient-melting shock pressures and impact velocities for these seven metals, are shown in Table 2.

For aluminum, beryllium, and iron, detailed Los Alamos tabulations of release temperature versus shock pressure are not available. However, for these three metals, an estimate of a complete equation of state has been obtained from Los Alamos.[*] This equation of state was fitted by Osborne to combined results of shock experiments which produced pressures on the order of a megabar, and theoretical statistical-mechanical relations which become valid at extremely high pressures, and has been successfully employed in the hydrodynamic calculation of hypervelocity-impact cratering in iron and aluminum.[7,8] However, in these calculations the energies, and hence temperatures, are not known with as much confidence as the other variables of the flow problem, and to symbolize this the aluminum curve in Fig. 3 is dashed. Therefore, the predicted shock-melting properties for these three metals are approximate values only. Table 3 presents these pressures and impact velocities based on the zero-pressure internal energies of incipient and complete melting given by Ref. 9, which is the primary source of melting temperatures and zero-pressure energies used in this study.

----

[*] Personal communication from F. Harlow, Los Alamos Scientific Laboratory.

Table 2

ESTIMATED INCIPIENT-MELTING PROPERTIES FOR SEVEN METALS

Material	Density (gm/cc)	Melting Temperature (°K)	Incipient-Melting Shock Pressure (Mb)	Impact Velocity (km/sec)		
				Similar Material	Iron Projectile	Aluminum Projectile
Cobalt	8.82	1768	2.4	6.1	6.3	9.3
Chromium	7.13	2170	2.4	6.6	6.6	9.5
Molybdenum	10.20	2890	2.7	6.0	6.6	9.8
Nickel	8.86	1728	2.3	5.8	6..	9.0
Titanium	4.51	1950	1.3	6.8	5.6	7.6
Vanadium	6.1	2190	1.8	6.6	6.1	8.7
Tungsten	19.17	3650	3.4	4.9	6.5	10.3

Table 3

APPROXIMATE SHOCK-MELTING PROPERTIES FOR
ALUMINUM, BERYLLIUM, AND IRON

Material	Density (gm/cc)	Melting Temperature (°K)	Shock Pressure (Mb)	Impact Velocity (km/sec)		
				Similar Material	Iron Projectile	Aluminum Projectile
Incipient Melting						
Aluminum	2.70	932	0.7	5.6	4.3	5.6
Beryllium	1.85	1556	1.5	11.4	8.2	10.5
Iron	7.84	1812	1.8	5.4	5.4	7.9
Complete Melting						
Aluminum	2.70	932	1.0	7.0	5.3	7.0
Beryllium	1.85	1556	1.9	13.1	9.4	12.0
Iron	7.84	1812	2.1	6.0	6.0	8.8

IV. ENERGY METHOD FOR CORRELATION OF INCIPIENT-MELTING IMPACT VELOCITIES

Since Los Alamos release-temperature and equation-of-state data are not available for all metals, an attempt was made to distill an approximate empirical correlation from the preceding results which would enable approximate prediction of incipient-melting impact velocities for other metals. This has been done by the following method.

In a one-dimensional impact between plates of similar materials, the specific internal energy initially produced in the shocked region is

$$e = \frac{1}{8} v^2 \tag{7}$$

where v is the relative impact velocity, provided the initial state of the plates is defined to have zero internal energy.[8] Equation (7) is compatible with Eq. (1) but is expressed in a different form.

The internal energy of material which is just at incipient melting under zero pressure is

$$H_m = \int_{T_o}^{T_m} C_p dT \tag{8}$$

where C_p is the specific heat.

For an impact velocity, V_m, which just causes the material to expand back to incipient melting, the fraction of the maximum initial internal energy which is left in the material by the irreversible losses of the shock as "heat" energy is just

$$f = \frac{H_m}{V_m^2/8} \tag{9}$$

Using the estimates of V_m for 19 metals in Tables 1 to 3, and published values of H_m,[9] the values of f for these 19 metals have been calculated and are shown in Table 4.

Table 4

APPROXIMATE FRACTION OF SHOCK ENERGY REMAINING IN METAL AS
"HEAT" ENERGY FOR THE CASE OF AN INCIPIENT-MELTING SHOCK

Metal	$H_m^{(9)}$ (j/gm)	$f = 8H_m/V_m^2$
Aluminum	672.1	0.17
Beryllium	3684	0.22
Cadmium	74.03	0.16
Chromium	1236	0.24
Cobalt	928.2	0.20
Copper	465.0	0.20
Gold	147.8	0.14
Iron	1053	0.30
Lead	41.32	0.16
Molybdenum	886.4	0.20
Nickel	811.9	0.20
Silver	246.2	0.19
Thallium	41.22	0.18
Thorium	310.6	0.26
Tin	51.84	0.17
Titanium	1173	0.21
Tungsten	557	0.19
Vanadium	1268	0.23
Zinc	167.3	0.18

Table 5

PREDICTED APPROXIMATE VALUES OF SIMILAR-MATERIAL
INCIPIENT-MELTING IMPACT VELOCITIES[a]

Metal	Density (gm/cc)	Melting Temperature (°K)	H_m (j/gm)	$V_m^{\pm 20\%}$ Predicted (km/sec)
Bismuth	9.79	545	33.96	1.2
Magnesium	1.74	923	738.5	5.4
Niobium	8.60	2770	795.0	5.6
Platinum	21.37	2043	273.5	3.1
Tantalum	16.46	3270	480.9	4.4
Uranium	18.7	1406	205.3	2.9

[a]Based on $f = 0.20$.

It is seen that for incipient-melting impacts, the fraction of shock internal energy which remains as internal energy at zero pressure is $0.20 \begin{Bmatrix} +.10 \\ -.06 \end{Bmatrix}$. It seems significant that this fraction is so constant, since the melting energies in this group of metals vary by almost two orders of magnitude. If one assumes that this empirical relation is valid for other metallic elements, it is possible to predict $V_{.n}$ from the known H_m. This has been done for six additional metals, and the results are shown in Table 5. The uncertainty in the predicted melting impact velocity based on the observed scatter in f is +19 per cent and -18 per cent.

In Table 1, the footnoted quantities at the complete melting condition for gold and copper were also obtained from this fraction f. That is, as the Los Alamos experimental shock pressures were not high enough to achieve complete melting for these metals, it was assumed that the value of f remained constant at the incipient-melting value (Table 4), and the complete-melting impact velocity was then obtained by calculating the fraction of shock-zone energy (Eq. (14)) which would just add the heat of fusion to the metals. This method was checked against the complete-melting values for the other seven metals in Table 1, and the agreement was always within 4 per cent.

V. INFLUENCE OF VAPORIZATION AND MELTING ON
HYPERVELOCITY CRATERING

As discussed in Ref. 8, the hypervelocity cratering process proceeds in two stages:

1. The shock generated on initial impact races through the target with diminishing intensity.
2. The material behind the shock then flows and generates the crater on a much longer time scale.

As a result, the material flow which generates the crater always occurs in a medium which has been conditioned by the shock, and it is this conditioning which we will now discuss.

As an example, consider the case of a square cylinder (length equals diameter) which moves along its axis and strikes a semi-infinite target at normal incidence. This problem has cylindrical symmetry, and we shall consider conditions along the axis of symmetry. Figure 5 shows the peak pressures produced by the shock along the axis as a function of depth. The units of depth are given in terms of the characteristic dimension of the projectile, d, and we shall call this the scaled depth.

The initial impact of aluminum on aluminum at 20 km/sec produces a pressure of about 4.9 Mb. This pressure persists along the axis to a scaled depth of about 0.7, at which time a rarefaction wave overtakes the shock. Under the influence of the rarefaction wave and the lateral expansion which also begins at that time, the shock pressure subsequently drops with about the -1.2 power of depth. At a scaled depth of 4.5, which is somewhat greater than the final crater depth given in Ref. 8, the peak shock pressure is about 0.5 Mb. Although the curve of Fig. 5 is terminated at this point, the shock does propagate beyond this depth and is in fact the agent which would cause spallation were it to encounter a free surface.

Also shown in Fig. 5 is an estimate of the temperature to which the target material comes upon expansion back to zero pressure after the shock has passed. At scaled depths less than 2.7 the material
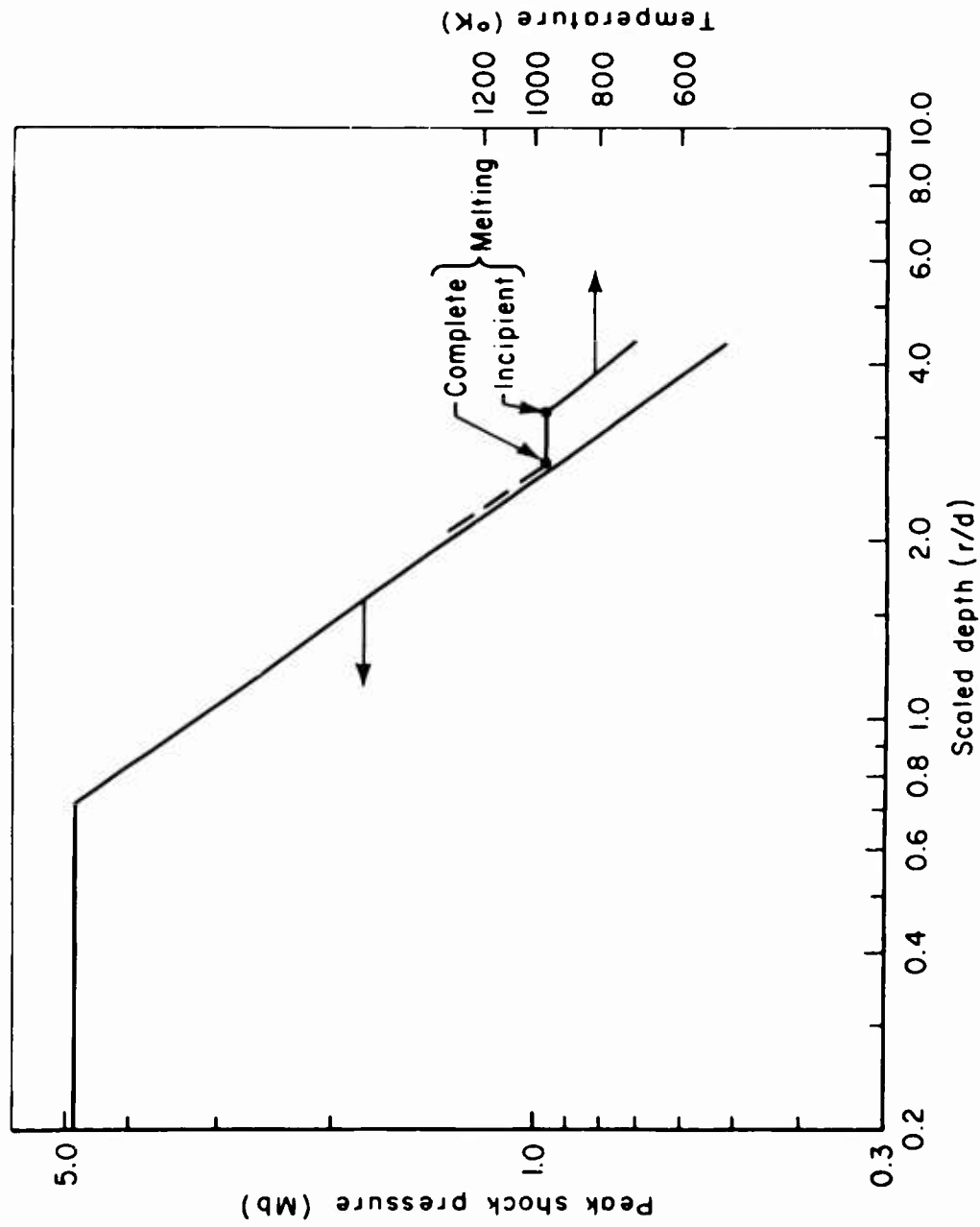
Fig. 5—Peak shock pressure and temperature after shock release as a function of depth along the axis for aluminum on aluminum at 20 km/sec

returns to a liquid state which is hotter than the melting temperature of $930^{\circ}K$. Between the scaled depths of 2.8 and 3.3 the material will be a mixture of solid and liquid, and below a depth of 3.3 it is a solid, heated to the temperature shown in the graph. These depths are seen to be significant in comparison with the final scaled crater depth of 4.0.

At the instant of time when the shock reaches a scaled depth of 2.8, the bottom of the forming crater is at a scaled depth of about 1.7. Consequently, the subsequent material flow is into a target having the temperature distribution shown in Fig. 5. Some important implications may be derived from these considerations:

1. The process is truly hydrodynamic to a scaled depth of 3.3, and below this the validity of the hydrodynamic approximation is enhanced by the fact that the target material has been intensely heated.

2. Theories which seek to include the role of material strength without including these heating effects seem doomed to failure at the higher velocities.

3. Those theories which attempt to assess the effects of material strength and viscosity by calculating their effects on the initial shock wave seem incorrectly oriented for two reasons: (a) The dynamic yield strength can have little effect on shocks of greater than 0.5 Mb, and (b) the viscosity of the actual material is orders of magnitude less than the artificial viscosities which are used in the numerical calculations, yet the inclusion of artificial viscosity still leads to the correct shock strength and position. Thus, reasonable values of dynamic yield strength and viscosity cannot have much influence on the initial shock in this problem. The important physical quantity is the strength of the material after conditioning by the front-running shock, and its influence will be felt in governing the material flow which finally forms the crater.

4. The "energetic" theories of hypervelocity cratering which assumed that all the projectile's kinetic energy was absorbed in bringing the crater and projectile material to exactly a state of fusion are seen to be on an incorrect physical basis. Figure 5 illus-

trates well the fact that a great deal of the crater material has been
given much more internal energy than is necessary to melt it. In fact,
at 72 km/sec an appreciable amount is vaporized. In general, the av-
erage specific internal energy imparted to the crater material increases
rapidly with impact velocity. Consequently, a penetration theory based
on energetics cannot lead to a "two-thirds law" (crater volume propor-
tional to projectile kinetic energy). When the increase of average
specific internal energy is taken into account, the value of two-thirds
will be reduced.

VI.   EFFECT OF TARGET MELTING ON CRATER SIZE

We will now compare the depths of the melted zones with the cra-
ter sizes predicted by the hydrodynamic theory. The zones of material
states for three different aluminum-aluminum impact velocities are plot-
ted in Fig. 6.[8] In this plot, peak particle velocity instead of peak
pressure, as shown in Fig. 5, is plotted versus depth. The two are
equally valid because the shock pressure may be expressed as a function
of only the change in particle velocity across the shock.

For the impact at 20 km/sec, it is seen that the target material
is melted to nearly the crater depth of 40 cm predicted purely on the
basis of hydrodynamic flow. Thus, at about this impact velocity, one
may expect that craters in all alloys of aluminum will have about the
same depth, since the material strength does not influence the shock
to a measurable degree at depths of less than 40 cm, and the melting
characteristics of the various commercial alloys are similar. At im-
pact velocities greater than 20 km/sec, the melted region will extend
below the predicted craters. For example, at 72 km/sec the melted re-
gion is seen to extend to about 78 cm, which may be compared with the
55-cm penetration predicted in Ref. 8.

Therefore, at impact velocities above 20 km/sec, the crater dimen-
sions are determined essentially by the extent of the melted region.
This is illustrated in Fig. 7. The numbers that are the basis for the
predicted crater modification should be considered preliminary estimates
which might be revised when a more thorough investigation is conducted.
To reflect this fact, the estimated crater depth is shown as a dashed
line in Fig. 7.

Figure 8 shows the material-state zones for the case of iron-iron
impacts   Just as in the case of aluminum, the melted zone becomes as
deep as the hydrodynamic-flow crater at an impact velocity of 20 km/sec.
At 72 km/sec, the melted zone in iron is 81 cm deep, compared to the
Ref. 8 penetration prediction of 45 cm.

Although the depths delineating the various state regimes may be
slightly revised in the future, these qualitative physical observations
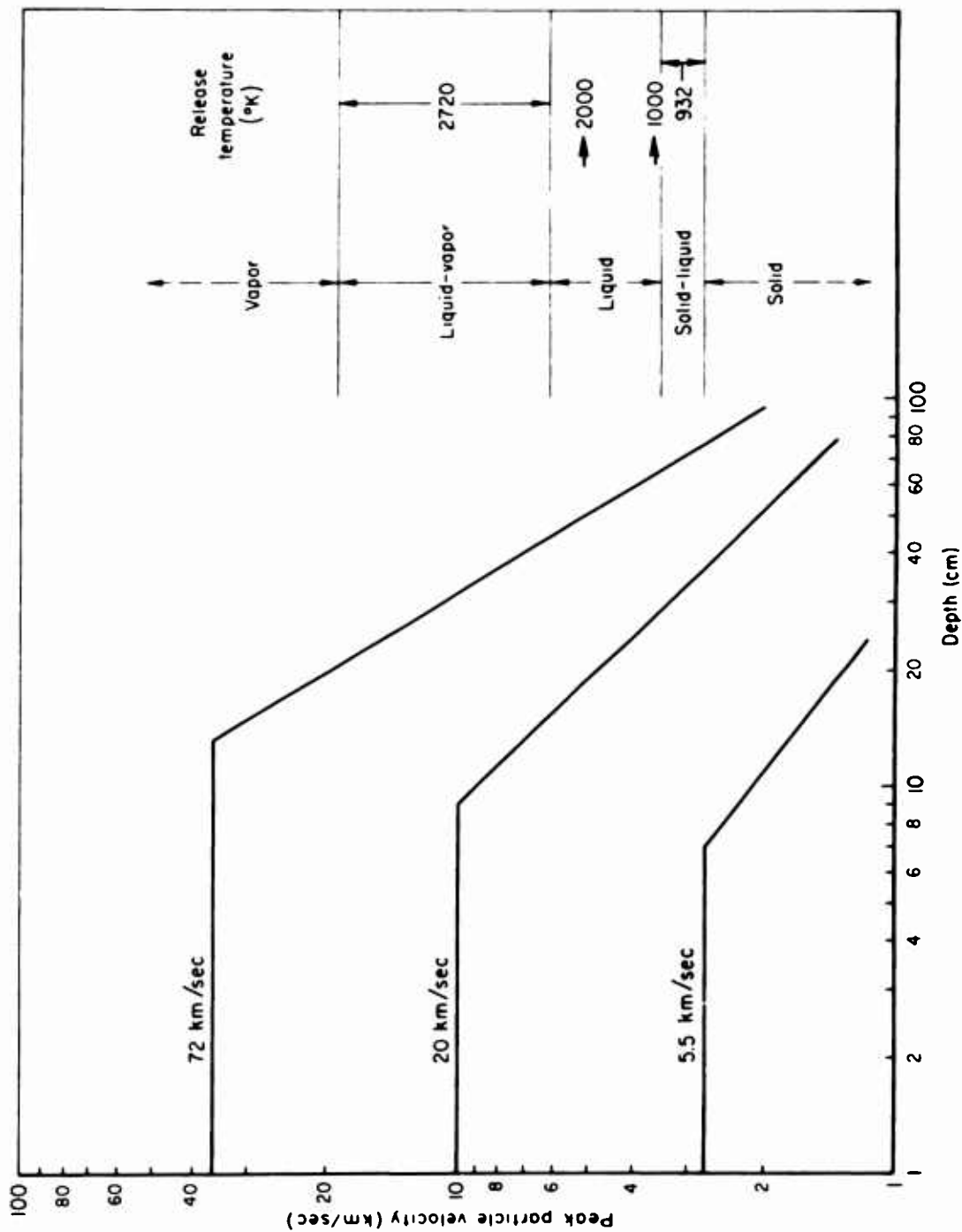are still expected to apply.

Fig. 6—Left scale: peak particle velocity as a function of depth along axis of symmetry for 10 x 10-cm aluminum cylinders striking end-on on semi-infinite aluminum targets. Right scale: release temperature and material state for same cases
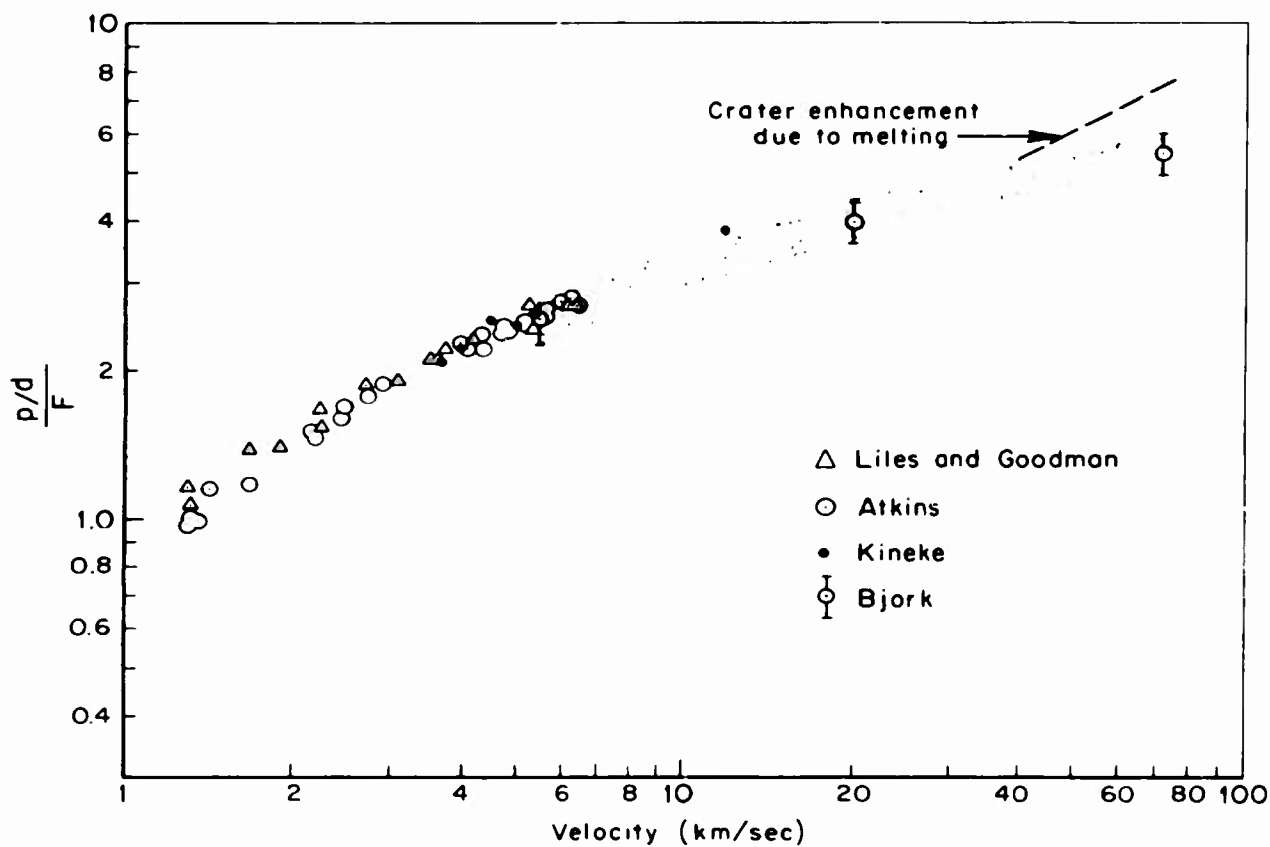
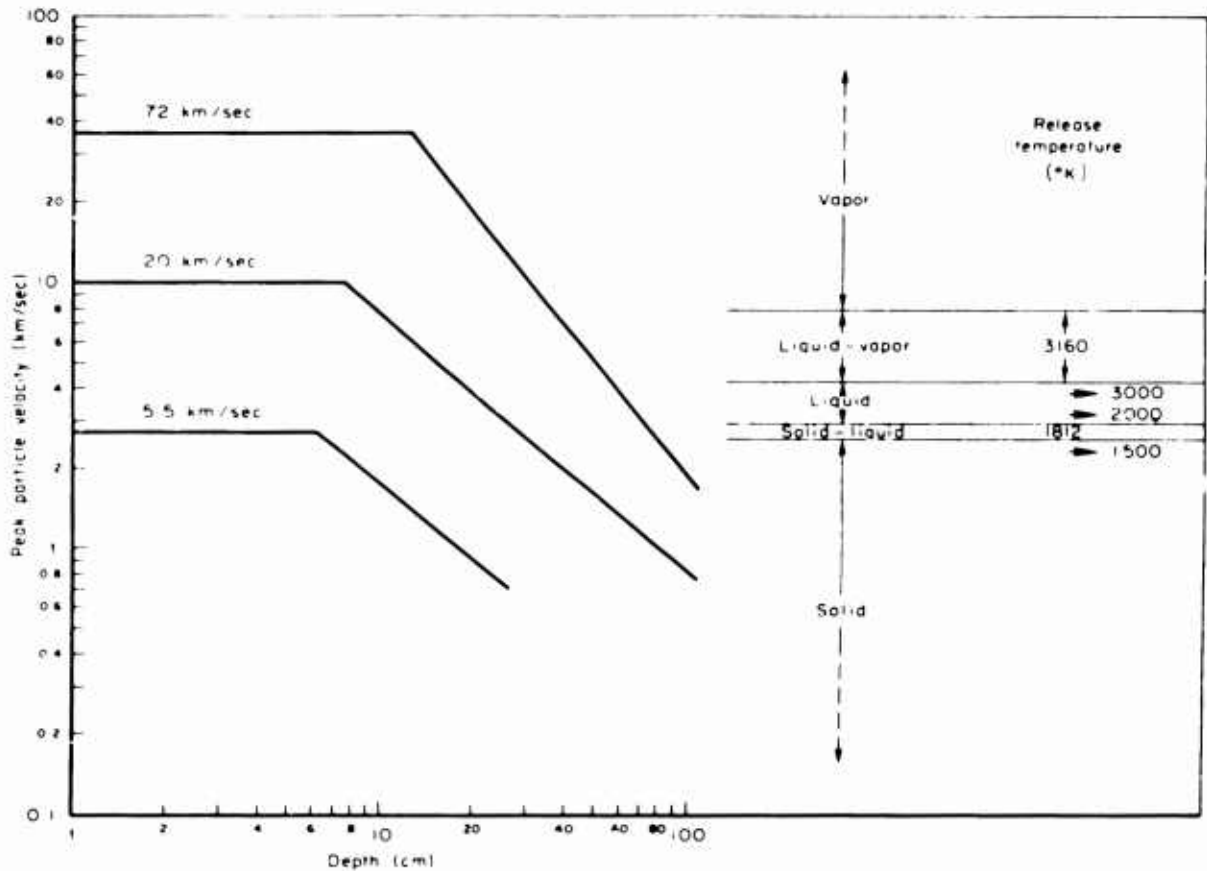Fig. 7— Dissimilar-material scaling law compared with experimental data for 1100-F aluminum targets[10]

Fig. 8—Left scale: peak particle velocity as a function of depth
along axis of symmetry for 10 x 10-cm iron cylinders
striking end-on on semi-infinite iron targets.
Right scale: release temperature and
material state for some cases

REFERENCES

1. Courant, R., and K. O. Friedrichs, _Supersonic Flow and Shock Waves_, Interscience Publishers, Inc., New York, 1948, p. 142.

2. Walsh, J. M., _et al._, "Shock-Wave Compressions of Twenty-Seven Metals. Equations of State of Metals," _Phys. Rev._, Vol. 108, No. 2, October 15, 1957, p. 196.

3. McQueen, R. G., and S. P. Marsh, "Equation of State for Nineteen Metallic Elements from Shock-Wave Measurements to Two Megabars," _J. Appl. Phys._, Vol. 31, No. 7, July 1960, p. 1253.

4. Rice, M. H., _et al._, _Solid State Physics, Advances in Research and Applications_, Vol. 6, Academic Press, Inc., New York, 1958.

5. Taylor, John W., "Residual Temperatures of Shocked Copper," _J. Appl. Phys._, Vol. 34, No. 9, September 1963, p. 2727.

6. Bjork, R. L., and A. E. Olshaker, _A Proposed Scaling Law for Hypervelocity Impacts Between a Projectile and a Target of Dissimilar Material_, The RAND Corporation, RM-2926-PR, May 1965.

7. Bjork, R. L., "Numerical Solutions of the Axially Symmetric Hypervelocity Impact Process Involving Iron (U)," in F. Genevese (ed.), _Proceedings of Third Symposium or Hypervelocity Impact_, Vol. II, Armour Research Foundation of Illinois Institute of Technology, Chicago, February 1959 (Secret).

8. Bjork, R. L., _Effects of Meteoroid Impact on Steel and Aluminum in Space_, The RAND Corporation, P-1662, December 16, 1958.

9. Stull, D. R., and G. C. Sinke, _Thermodynamic Properties of the Elements_, American Chemical Society, Washington, D.C., 1956.

10. Bjork, Robert L., _Review of Physical Processes in Hypervelocity Impact and Penetration_, The RAND Corporation, RM-3529-PR, July 1963.